(Received 16 June 2025, Accepted 26 August 2025, Scheduled 17 October 2025)

Machine Learning Assisted Monopole Antenna Optimization Using EONNC and SFIS Algorithm for Wearable Applications

Rajendran Ramasamy[1], Samidoss Chinnapparaj[2], Vellaichamy Rajavel[3,*], Venkatesh P. Ravichandran[1], Abbas A. Farithkhan[4], and Amanulla Y. Jenifer[5]

[1] *Ramco Institute of Technology, Tamilnadu, India*
[2] *Department of Electronics Engineering (VLSI Design and Technology) Kalaignarkarunanidhi Institute of Technology, Coimbatore, India*
[3] *Mepco Schlenk Engineering College, Sivakasi, India*
[4] *Vel Tech Rangarajan Dr. Sagunthala R&D Institute of Science and Technology, India*
[5] *Sethu Institute of Technology, Kariapatti, India*

ABSTRACT: This paper examines the optimisation of antenna parameters for wire monopole, vertical trapezoidal monopole, and circular disc monopole antennas with Enhanced Optimizable Neural Network Classifier (EONNC) and Sugeno Fuzzy Inference System (SFIS). This study includes both quantitative and conventional antenna design techniques, offering comprehensive insights into antenna optimisation tactics. An advanced antenna selection algorithm identifies the ideal antenna by a comprehensive examination of performance metrics with EONNC, hence reinforcing the rigour of our research process. The geometric parameters of antennas are delineated, with SFIS proficiently ascertaining appropriate dimensions. EONNC categorises antennas into three classifications, whereas SFIS determines optimal parameters for estimating antenna size. Accuracy measures assess EONNC performance, whereas SFIS performance is measured using Mean Squared Error (MSE) and Mean Absolute Percentage Error (MAPE). Our suggested technique demonstrates remarkable precision in parameter prediction and antenna classification, with a mean absolute percentage error (MAPE) of less than 4% and an accuracy exceeding 99.3%. The research examines a circular disc monopole antenna due to limitations in simulation duration for SAR measurements, resulting in SAR values of 0.978 W/kg for arm measurements and 0.985 W/kg for hand measurements. The proposed techniques are very relevant to actual antenna designs, especially for wearable applications.

1. INTRODUCTION

Wireless communication has made wideband and high-gain antennas necessary. Due to its cost-effectiveness, small form, and wide frequency range, monopole antenna appears promising. Many printed monopole antennas have been produced, but their gain is limited. Numerous experiments have been conducted to enhance printed monopole antennas, including modifications to the ground plane, Artificial Magnetic Conductor (AMC) integration, and Frequency Selective Surface (FSS). Wearable tech has grown rapidly, drawing scientific curiosity. These technologies offer solutions for various industries, including sports, military, medicine, entertainment, healthcare, and education. The design must also meet Federal Communications Commission (FCC) safety standards for wearable electronics. These difficulties can be addressed with proper design. Unidirectional antennas or isolators can improve performance and minimise Specific Absorption Rate (SAR). Due to its widespread use in healthcare, sports, child monitoring, and consumer electronics, wearable technology has received scientific attention. These devices need Wi-Fi capability to work smoothly. Wearable technology developers face a significant challenge in designing antennas that are wearable, flexible, durable, cost-effective, and perform as well as traditional copper antennas.

For Long Range (LoRa) applications, Yahya et al. presented a compact monopole antenna using a machine-learning method. The proposed antenna operates in two frequency bands, and Gaussian Regression algorithm was employed to estimate the resonance frequency accurately. Furthermore, the proposed method yields a favourable radiation pattern and maximum gain [1]. Rizwan et al. suggested a textile monopole antenna that utilizes machine-learning techniques to monitor the healing of bone fractures. The suggested antenna was designed to function in the ultra-wideband (UWB) frequency range employed in wearable technology [2]. Zheng et al. proposed a dual-monopole antenna that employs machine learning techniques. They developed a Gaussian process optimization approach to enhance efficiency and decrease computation time. This approach was used to generate a broad frequency band [3]. Huang et al. suggested an Mean Absolute Error (MAE) decoupling design based on machine learning algorithms. They developed a k-means algorithm to improve antenna isolation and optimize the antenna decoupling structure [4]. Ramasamy and Bennet devised a machine-learning approach for estimating antenna parameters that are both effective and efficient. They created Direct Torque Control (DTC) and Fuzzy Inference System (FIS) algorithms for antenna classification and parame-

* Corresponding author: Vellaichamy Rajavel (rajavel572@gmail.com).

ter estimation. The proposed approach achieves high accuracy with minimal calculation time [5, 6]. Sharma et al. proposed a monopole antenna that utilizes machine-learning techniques, making it suitable for dual-band applications. They developed several machine-learning approaches for determining the optimal antenna design parameters efficiently [7]. Sharma et al. utilized machine learning (ML) techniques, specifically Gaussian process (GP) regression and Artificial Neural Networks (ANNs), to model and optimize three-dimensional printed dielectric distributions surrounding monopole antennas. This approach substantially decreased computational expenses (by 80–97%) while facilitating effective inverse design for beam shaping, culminating in the successful experimental validation of a three-beam prototype [8]. Wu et al. suggested an Antenna Geometry Design (AGD) that utilizes an automated algorithm. They developed the ML-AO (Assisted Optimization) algorithm to enhance the accuracy of the antenna geometry design and reduce the mutual coupling between antenna components [9]. Shah et al. designed textile antennas using various machine-learning algorithms. They developed the K-Nearest Neighbor (KNN), Random Forest Regressor (RFR), and Deep Neural Network (DNN) algorithms to enhance optimization, increase bandwidth, and reduce computation time without compromising accuracy [10].

A sickle-shaped AMC structure and a low-profile UWB antenna were proposed by Pandi Ravichandran and Velayudham to enhance on- and off-body communication performance. Its impedance bandwidth, radiation efficiency, and SAR reduction make it ideal for wearable and body-centric wireless systems [11]. Nakmouche et al. proposed an FSS-reflected monopole antenna based on a machine-learning approach, aiming to enhance gain and radiation efficiency, minimize computational time, and reduce antenna size [12]. Choo et al. suggested a bent monopole antenna utilizing a DNN-based machine learning system and evaluated Mean Square Error (MSE) and R-squared values. The proposed techniques aim to increase precision, achieve good impedance matching, and optimize ground size while also reducing manufacturing errors in bending angles and length [13]. Shi et al. provided the best antenna geometry parameters using a machine learning technique, which involved using a Support Vector Machine (SVM) classification and stacking ensemble framework to estimate several antenna parameters, including accuracy, efficiency, and ideal antenna geometry parameters [14]. Ganesh and Chaturvedi presented a wearable monopole array antenna for breast cancer diagnosis, which utilizes Rogers RT5880 material with a thickness of 0.51 mm and a resonance frequency of 3.7 GHz. The proposed antenna offers strong isolation and good SAR, making it suitable for tumour detection [15]. Zhao et al. proposed a dual-monopole antenna for biomedical healthcare applications, which encompasses several key parameters, including SAR, S_{11}, gain, and radiation pattern [16]. Saad et al. proposed a monopole antenna that operates in the 2.45 GHz frequency spectrum for wearable applications, utilizing an AMC surface made of cotton cloth to reduce body radiation absorption and increased gain [17]. Sam et al. proposed a circular monopole antenna that operates at the UWB frequency spectrum for use in wearable biomedical applications. They developed an Electromagnetic Band Gap (EBG) structure using 0.7 mm-thick denim textile. The suggested EBG structure comprises a 2×2 array antenna that enhances gain, directivity, frequency response stability, and SAR [18]. Abdelghany et al. proposed a dual-band textile antenna for wearable applications. The proposed monopole antenna features a denim textile substrate and a broad frequency spectrum, with optimal performance in SAR, flat, and bending configurations [19]. Chatterjee and Kundu use SVM and ANN algorithms to build a spiral-shaped multiband monopole antenna for MICS and IEEE 802.11a/b applications [20]. Yahya et al. present a machine learning-optimised wearable antenna for LoRa-based localisation, utilising Random Forest and Support Vector Machine to enhance design efficiency and positioning accuracy [21]. In this experimental study, Hamdi and Balti construct smart antenna sensor networks and simulate energy consumption management for intelligent Internet of Medical Things (IoMT) systems [22]. This work describes a machine learning-based approach to antenna design and improvement. It features a spiral-shaped multiband monopole antenna for MICS and IEEE 802.11a/b, supported by Support Vector Machine and Artificial Neural Network, as well as a superior LoRa-based localisation wearable antenna utilising Random Forest and SVM. It also explores the experimental building of smart antenna sensor networks and the management of energy utilisation for smart IoMT systems. A comprehensive examination of the existing literature has recently been undertaken, yielding findings that suggest that while numerous researchers have successfully developed machine learning models capable of accurately classifying different types of antennas, relatively few have endeavoured to estimate antenna characteristics following classification.

Furthermore, these models often compromise the calculation performance, and the precision of parameter estimation can still be improved. The proposed (EONNC + SFIS) method employs an enhanced optimizable neural network classifier to categorize the three primary types of antennas wire monopole, vertical trapezoidal monopole, and circular disc monopole, and utilizes Sugeno fuzzy inference systems to forecast antenna parameters. Fuzzy inference algorithms can accurately estimate the monopole antenna height and pin height for wire monopoles, circular disc monopoles, and vertical trapezoidal monopole antennas while minimizing processing time.

2. PROPOSED METHODOLOGY

Figure 1 illustrates the suggested intelligent antenna synthesis system. HFSS (High-Frequency Structure Simulator) toolbox facilitates the establishment of a database for diverse antennas by specifying parameters such as dimensions, frequency, gain, S_{11}, bandwidth, monopole height, pin height, and material characteristics. Thereafter, the HFSS produces geometric models, meshes the structures, conducts simulations to assess performance metrics such as radiation patterns and impedance, executes the simulations, retrieves relevant data through post-processing, and organises the data into a structured database. Enhanced Optimizable Neural Network Classifier, a robust and adaptable machine learning model, optimises its parameters to enhance the performance in classification tasks. Neural net-

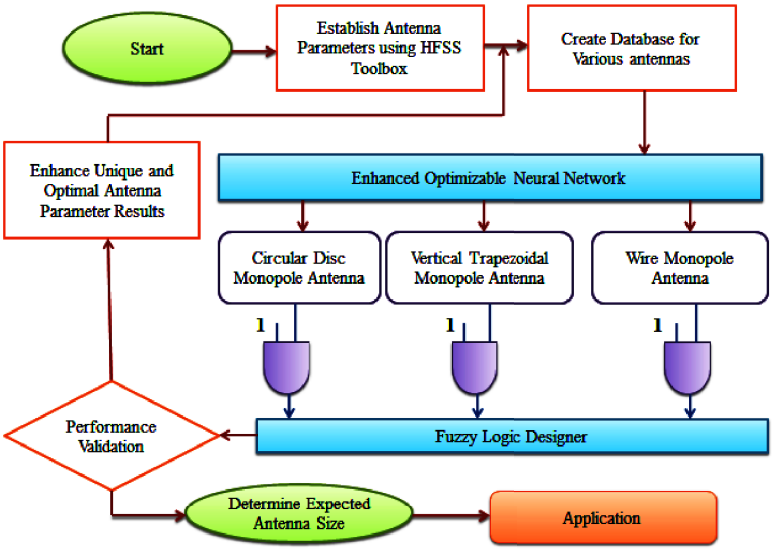

FIGURE 1. Overview of proposed intelligent antenna synthesis system.

works can utilise this principle in antenna design to optimise the parameters of various configurations. For example, by examining antenna designs such as Circular Disc Monopole Antenna, Vertical Trapezoidal Monopole Antenna, and Wire Monopole Antenna, the Enhanced Optimizable Neural Network classifier can be trained to understand the correlations between antenna parameters and performance metrics, including S_{11}, gain, radiation patterns, bandwidth, and impedance matching.

The classifier can subsequently utilise optimisation techniques to iteratively adjust these parameters to enhance the target antenna performance criterion. When EONN correctly predicts the antenna, the output of a specific class becomes one, and the output of the other classes becomes zero. Upon receiving the EONNC output, the AND gate assesses if both inputs are identical prior to triggering the SFIS. The optimal antenna size parameters for the associated input design parameters, such as the bandwidth (GHz), operating frequency (GHz), gain (dB), and reflection coefficient (dB), are supplied by datasets stored in the SFISs. The process of identifying the optimal pin and monopole height parameters involves using SFIS, which is tested with a specific design parameter, and the results are compared with the saved datasets. This method leverages the adaptability and flexibility of neural networks to rapidly explore an extensive design space, potentially leading to the discovery of novel antenna engineering solutions and improved antenna performance.

3. METHODS DESCRIPTION

3.1. Wire Monopole Antenna

Figure 2 illustrates the proposed monopole antenna. A wire monopole antenna, an essential component in radio transmission, consists of a solitary conducting wire, often positioned vertically, with one end either grounded or left open and linked to the transmitter or receiver. It is suitable for terrestrial installations where signals need to be transmitted or received in all directions horizontally due to its straightforward design and vertical orientation, which enable omnidirectional radiation. The length of an antenna, typically a multiple or percentage of the radio frequency wavelength, affects its performance. Wire-monopole antennae are commonly utilized in wireless communication systems owing to their straightforward design, ease of deployment, and extensive coverage. These antennae are widely used in various applications, including AM and FM radio broadcasting, mobile communication systems, wearable devices, and Radio Frequency Identification (RFID).

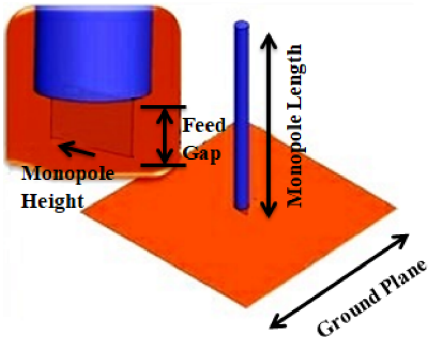

FIGURE 2. Wire monopole antenna.

In Equation (1), the height (length) of the monopole antenna is represented by variable L. Additionally, the speed of light in the medium is represented by constant c, and variable f represents the resonant frequency of the antenna.

$$L = \frac{c}{4f} \tag{1}$$

The result of an electrically short monopole's gain over an infinite plane is expressed by Equation (2).

$$G(\theta, \phi) = \eta_r \eta_m D(\theta, \phi) \tag{2}$$

where $D(\theta, \phi)$ is the antenna directivity, and η_r, η_m are the radiation and mismatch efficiencies given by Equations (3)

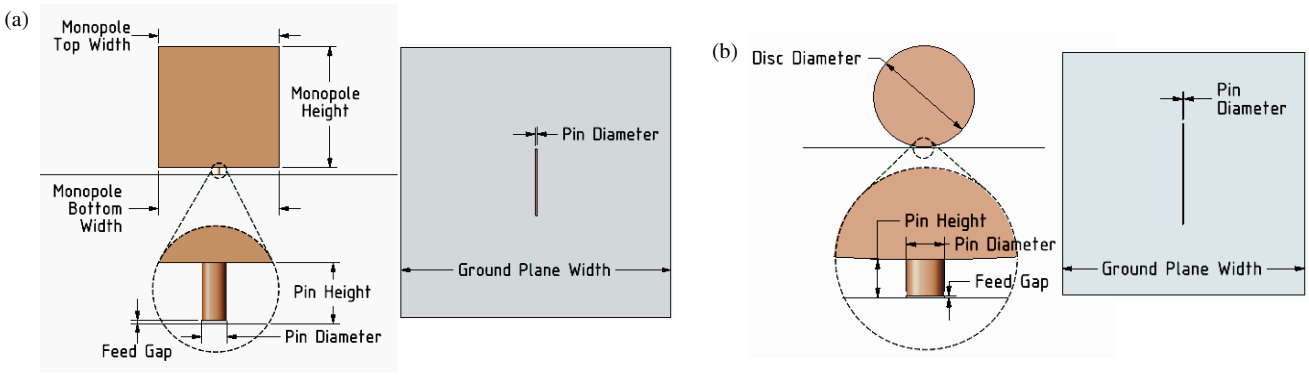

FIGURE 3. (a) Vertical trapezoidal monopole antenna. (b) Circular disc monopole antenna.

and (4)

$$\eta_r = \frac{P_r}{P_r + P_L} \tag{3}$$

and

$$\eta_m = 1 - |\Gamma|^2 \tag{4}$$

3.2. Vertical Trapezoidal Monopole Antenna

The vertical trapezoidal monopole antenna, seen in Figure 3(a), exemplifies a distinct version of the monopole antenna design. In contrast to traditional wire monopoles, which generally have a straight vertical conductor, a trapezoidal monopole antenna exhibits a configuration akin to a trapezium. The purpose of this shape modification is to enhance particular performance attributes, including bandwidth, gain, radiation pattern, and impedance matching. The distribution of currents along the trapezoidal configuration of the antenna may influence its radiation pattern and impedance characteristics. This form of antenna is frequently employed in radar systems, wearable technology, wireless communication systems, and antenna arrays when the precise control of parameters is necessary. Designing and optimising a vertical trapezoidal monopole antenna necessitates the consideration of its geometric dimensions, material composition, and operating frequency to get appropriate performance metrics. For 2.4 GHz operation, the trapezoidal monopole antenna was designed with a lower base width of 75 mm, an upper base width of 25 mm, and a height of 31.25 mm. These dimensions were selected to provide a smooth impedance transition and to ensure resonance near the desired frequency, following standard monopole height guidelines (approximately $\lambda/8$).

3.3. Circular Disc Monopole Antenna

The circular disc monopole antenna depicted in Figure 3(b) is commonly used in various wireless communication applications. The circular disc serves as a radiating element, positioned perpendicular to the ground plane, which functions as the counterpoise. This antenna design is particularly suitable for situations where compactness and omnidirectional radiation are required, such as RFID, wearable technology, wireless sensor networks, and mobile communication devices [23]. The circular disc form allows for a broad bandwidth and straightforward construction, making it suitable for a wide range of frequencies. The ground plane beneath the circular disc enhances the antenna's performance by providing a stable reference plane and increasing radiation efficiency. By varying the size of the ground plane and disc, the circular disc monopole antenna can operate over a broad frequency range, making it a versatile option for various wireless communication and wearable applications. The circular disc monopole antenna was designed with a ground plane diameter of approximately 40 mm, chosen to be slightly less than half of the wavelength at 2.4 GHz to support efficient radiation and proper image current formation. These dimensions were finalized based on simulation results to achieve optimal impedance matching and radiation performance.

4. DISCUSSION OF RESULTS

4.1. Enhanced Optimizable Neural Network Classifier

Wire-monopole antennas are a common choice for wireless communication installations owing to their excellent coverage, simplicity, and ease of deployment. Unlike a regular wire monopole, which typically has a straight vertical conductor, a trapezoidal monopole antenna was formed like a trapezoid. Enhancing impedance matching, radiation pattern, bandwidth, gain, and other antenna performance parameters is the goal of this shape alteration. When a monopole antenna is erected, the radiating element is typically a circular disc positioned perpendicular to the ground plane. This antenna design is widely used in systems such as RFID, wearable technology, wireless sensor networks, and mobile communication devices, where omnidirectional radiation and compactness are necessary. Its round disc design allows for a wide bandwidth and relatively simple construction, making it suitable for a range of frequencies. Table 1 lists the anticipated performance metrics for each antenna.

A table presenting the confusion matrix for the classification system is shown in Figure 4(a). This matrix illustrates the model's performance in classifying antennas by comparing the expected and actual classes. The total number of columns in the matrix, which indicates the number of predictions for each class, represents the number of predicted values for each class. It is evident from the matrix that every diagonal grid number is visible, indicating that every antenna operates as intended.

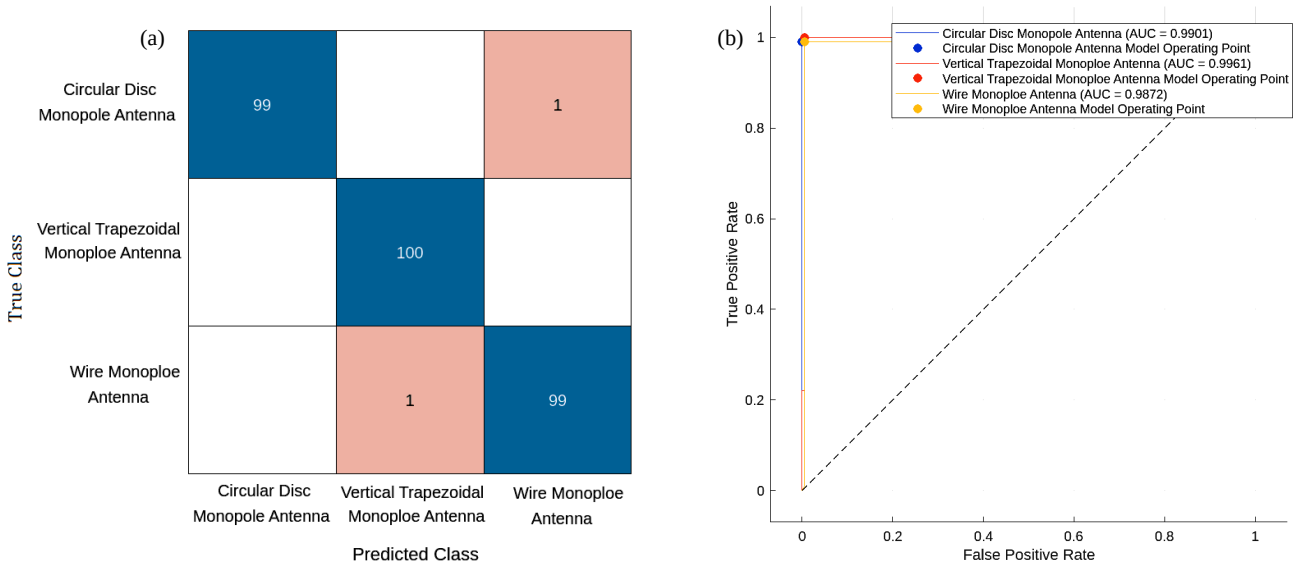

FIGURE 4. (a) Proposed confusion matrix. (b) Region of curve plot.

TABLE 1. Antenna performance parameters.

Parameters	Circular Disc Monopole Antenna	Vertical Trapezoidal Monopole Antenna	Wire Monopole Antenna
Reflection Coefficient (dB)	-11.664dB to -31.12dB	-10.13dB to -28.978dB	-12.12dB to -30.18dB
Resonant Frequency (GHz)	1GHz-7GHz	2GHz-5GHz	2.4GHz-5GHz
Gain(dB)	2dB-8dB	2dB-4dB	1dB-2dB
BW(GHz)	0.12GHz-2GHz	0.1GHz-0.906GHz	0.12GHz-1.024GHz

Figure 4(b) shows the Receiver Operating Characteristic (ROC) curve, which provides information about the classifier's performance. An ROC curve close to one indicates better than predicted categorization performance. The area under the curve for the wire monopole antenna was 0.9872; that for the circular disc monopole antenna was 0.9901; and that for the vertical trapezoidal monopole antenna was 0.9961.

The subsequent table delineates a comparison between the Optimizable KNN classifier (OKNNC) and Enhanced Optimizable Neural Network Classifier regarding performance metrics. Both classifiers exhibited commendable performance; yet, there were some subtle distinctions between them. Table 2 indicates that the Enhanced Optimizable Neural Network Classifier requires 13.255 seconds for training, but the OKNN classifier necessitates 14.327 seconds, which is marginally longer. These training times were measured on a standard workstation equipped with an Intel i5 processor, 8 GB of RAM, and no dedicated GPU acceleration. This demonstrates that both models are computationally efficient and feasible to train using moderate hardware resources. However, the Enhanced Optimizable Neural Network Classifier can predict around 7000 observations per second, while the OKNN classifier can predict approximately 8000 observations per second.

The Enhanced Optimizable Neural Network Classifier surpassed the OKNN classifier in classification accuracy, achieving 99.3% compared to 99.16%. The Enhanced Optimizable Neural Network Classifier exhibits enhanced specificity and elevated true favourable and accurate negative rates, indicating improved accuracy. Both classifiers demonstrated flawless sensitivity and no false negatives, indicating their ability to identify all positive examples precisely without any omissions. Nonetheless, the Enhanced Optimizable Neural Network Classifier's marginally elevated false positive count of 2, in contrast to the OKNNC, should be taken into account while assessing the particular needs of the application. While both classifiers exhibit commendable performance, Enhanced Optimizable Neural Network Classifier has somewhat superior accuracy and specificity, potentially rendering it more appropriate for jobs requiring high classification precision.

The five-step procedure for creating the monopole susceptibility map in Figure 5 is systematic and thorough. HFSS software was initially employed to generate theme parameter maps for monopole antenna design. The maps are subsequently sampled utilising antenna inventories to gather data, which is saved in a dataset. The dataset was partitioned into two segments: training data (80%) and validation data (20%). The training

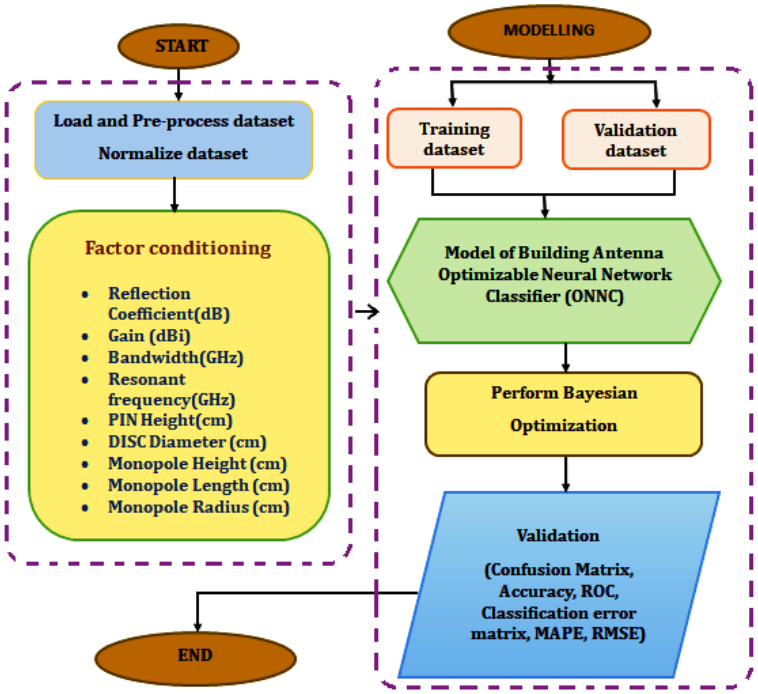

FIGURE 5. Flowchart for enhanced optimizable neural network classifier.

TABLE 2. Performance comparison of optimizable KNN classifier and enhanced optimizable neural network classifier.

S.No	Parameters	OKNN classifier	EONN Classifier
1.	Training Time (sec)	14.327	13.255
2.	Prediction Speed (observation/sec)	~ 8000	~ 7000
3.	True positive value	40	100
4.	True negative value	79	198
5.	False Positive value	1	2
6.	False Negative value	0	0
7.	Accuracy (%)	99.16	99.3
8.	Sensitivity (%)	100	100
9.	Specificity (%)	98.75	99

and validation datasets comprise 1,800 samples, with 600 samples for each antenna type: wire, vertical trapezoidal, and circular disc. For each antenna type, 100 samples were generated by varying six key antenna parameters. Dataset diversity was ensured by systematically adjusting antenna dimensions, substrate materials, and operating frequency ranges. These variations enable the dataset to capture a wide range of electromagnetic behaviours, support robust model training, and reduce the risk of overfitting.

The training data were utilised to create and evaluate models and maps, including the Fine Tree, Optimizable KNN, Optimizable SVM, and DTC models. The parameters obtained from the training data comprise gain, resonant frequency, and patch size. The validation procedure utilises diverse methodologies, including confusion matrices, ROC analysis, area under the curve (AUC) values, and classification error matrices. Antenna susceptibility maps are generated utilising indices from model development that evaluate antenna vulnerability and classify them as wire monopoles, vertical trapezoidal monopoles, and circular disc monopoles through Neural Networks. This technique enhances antennas through the application of Enhanced Optimizable Neural Network methodologies.

A negligible classification error is evident in the data presented in Figure 6(a). An error arises when the observed values deviate from the intended values. A positive mistake occurred when the disparity between the anticipated and actual values exceeded the prior value. To create a plot with minimal classification error for antenna classification, it is essential first to compile a dataset comprising diverse antenna types and extract pertinent information, such as dimensions and materials.

Upon training a classification model with this data, the model's performance may be assessed on an independent testing set to ascertain the classification errors for each antenna type. The errors can thereafter be graphed according to the antenna type, facilitating the recognition of patterns and problematic classifications. By systematically refining the model's architecture or feature selection based on plot insights, the accuracy and reliability of antenna classification systems can be enhanced. Figure 6(b) illustrates the SFIS employing a Sugeno Controller. A Sugeno-type 2 fuzzy logic system defines linguistic variables and membership functions to illustrate the impact of each input parameter on the system. This allows for the

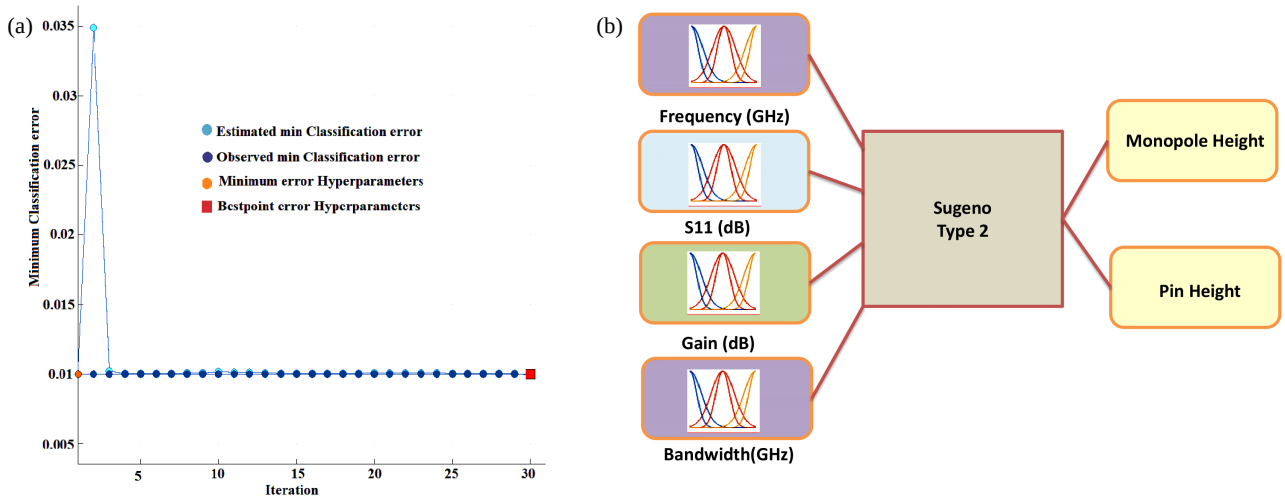

FIGURE 6. (a) Minimum classification error plot. (b) SFIS system using Sugeno controller.

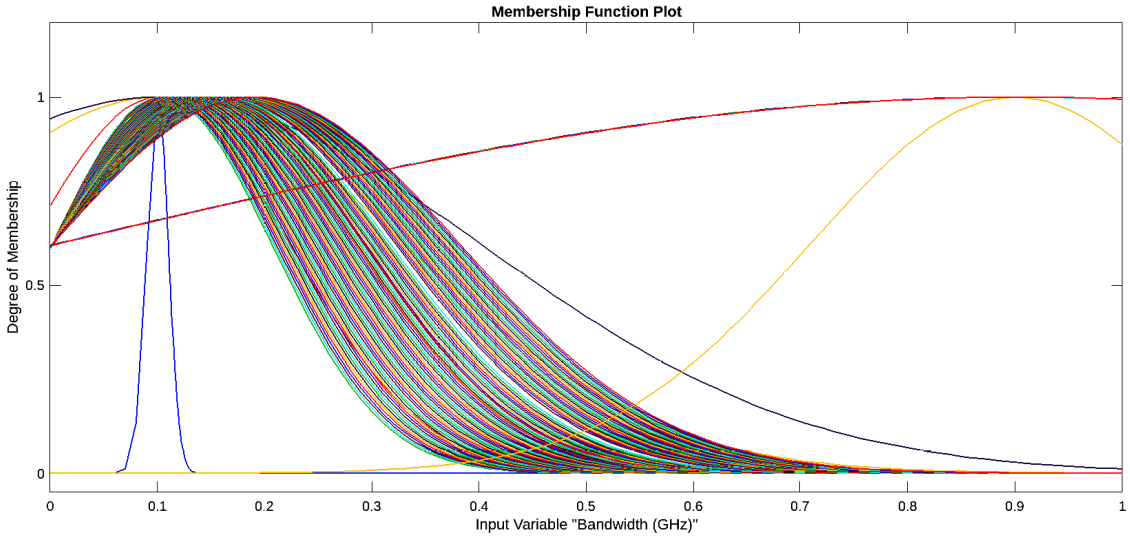

FIGURE 7. Gaussian membership function for bandwidth.

estimation of monopole antenna height characteristics, including pin height and monopole height, based on input features such as gain, frequency, S_{11}, and bandwidth. Linguistic factors categorise gain, frequency, S_{11}, and bandwidth into low, medium, and high levels, whereas membership functions delineate their respective levels of influence. Membership functions delineate the levels of output parameters, such as pin height and monopole height, and articulate them linguistically. The system employs a weighted average of input attributes and fuzzy algorithms to ascertain the outputs for monopole height and pin height.

A key component of fuzzy logic systems is Gaussian membership function, which demonstrates the extent to which a given input is associated with a specific scientific variable. It is represented as a bell-shaped curve, with the mean position in the centre and the standard deviation determining the spread. Gaussian membership function can be quantitatively represented by Equation (5).

$$\mu(x) = e^{-\frac{(x-c)^2}{2\sigma^2}} \tag{5}$$

x represents the input variable.

c is the centre or mean of the Gaussian.

σ is the standard deviation, determining the spread of the curve.

$\mu(x)$ denotes the degree of membership of x in the fuzzy set described by the Gaussian function.

The Gaussian function exhibits a maximum at position c, with its values diminishing proportionally as x diverges from this point. Gaussian function is a versatile tool for modelling complex systems and decision-making processes due to its ability to represent the uncertainty or vagueness inherent in variables associated with language inside fuzzy-logic systems.

Figure 7 depicts Gaussian membership functions for bandwidth, created using MATLAB to represent fuzzy sets, including narrow bandwidth, medium bandwidth, and large bandwidth. By graphing the membership values obtained by the Gaussian membership function, one may discern the relationship between various bandwidth values and each fuzzy set.

TABLE 3. Result analysis of Sugeno fuzzy inference system.

	Circular Disc Monopole Antenna		Vertical Trapezoidal Monopole Antenna		Wire Monopole Antenna	
	Disc Diameter (mm)	Pin Height (mm)	Monopole Height (mm)	Pin Height (mm)	Monopole Radius (cm)	Monopole Length (cm)
MAPE	4.42%	2.43%	3.84%	3.89%	4.14%	4.23%
RMSE	12.06%	7.79%	7.78%	8.84%	8.78%	9.12%
MAPE(Average)	3.425%		3.865%		3.685%	

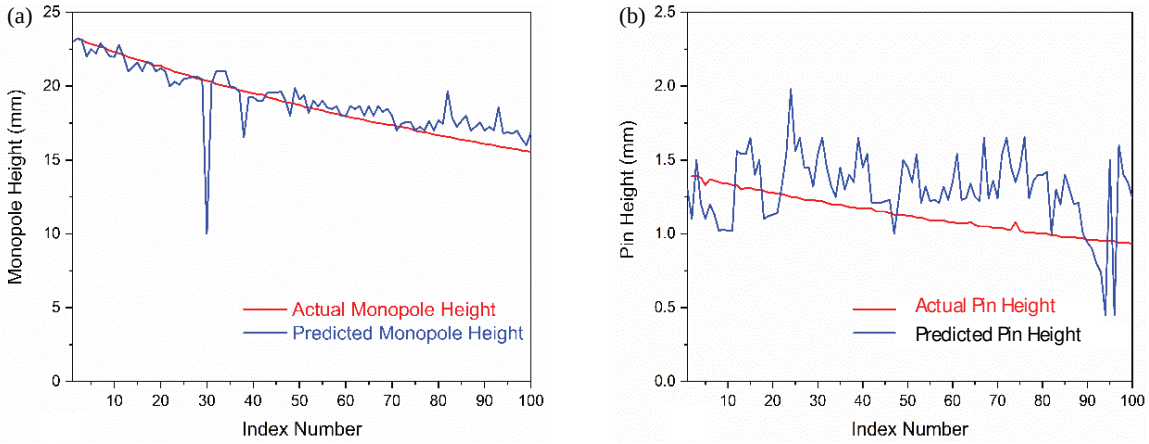

FIGURE 8. (a) Comparison between predicted and actual values of monopole height (cm). (b) Comparison between predicted and actual values of Pin height (cm).

Similarly, Gaussian membership functions for S_{11}, resonant frequency and gain were created.

The proposed model for the performance of the Vertical Trapezoidal Monopole Antenna is evaluated in the ruler view of tested sample [6]. The sample under examination is assessed according to specific geometric specifications, featuring a monopole height of 16.92 mm and a pin height of 1.01 mm, which yield a resonant frequency of 3.31 GHz, a gain of 1.27 dB, a bandwidth of 0.182 GHz, and an S_{11} of -18.5 dB. In contrast, the anticipated geometric parameters for the identical antenna are a pin height of 1.01 mm and a monopole height of 16.8 mm. The properties of the circular disc monopole antenna and wire monopole antennas are evaluated.

Table 3 presents the Mean Absolute Percentage Error and Root Mean Square Error, represented by Equations (6) and (7), respectively and utilised to evaluate the model's performance during testing.

$$\text{MAPE} = \frac{100}{n}\sum_{i=1}^{n}\left|\frac{X_i - Y_i}{Y_i}\right| \tag{6}$$

$$\text{MSE} = \frac{1}{n}\sum_{i=1}^{n}(X_i - Y_i)^2 \tag{7}$$

Figure 8(a) shows the comparison between predicted and actual values of monopole height (cm). Figure 8(b) shows the comparison between predicted and actual values of Pin height (cm). The application of a trained model is crucial for evaluating the efficacy of the proposed model, as illustrated in Figure 1. The circular disc monopole antenna must meet precise performance specifications, including S_{11} (-34.92 dB), gain (8.03 dB), bandwidth (1.02 GHz), and resonant frequency (2.85 GHz), with dimensions of 20.526 mm in disc diameter and 0.41 mm in pin height.

The proposed model features a disc diameter of 20.536 mm and a pin height of 0.42 mm. A simulation is performed utilizing the target parameters and synthetic geometric parameters to examine the characteristic parameters of each of the three antennas. Figure 9(a) illustrates a comparison of S_{11} curves, whereas Figure 9(b) presents S_{11} curves produced by the simulation.

SAR was estimated using a human arm phantom from ANSYS HFSS component library and an input power of 100 mW for the antenna, as described in [24, 25]. Figures 10(a) and (b) show an HFSS circular disc monopole antenna for SAR hand and arm measurements. The SAR arm and hand measurements yielded values of 0.978 W/kg and 0.985 W/kg, respectively. Therefore, only the circular disc monopole antenna was sim-

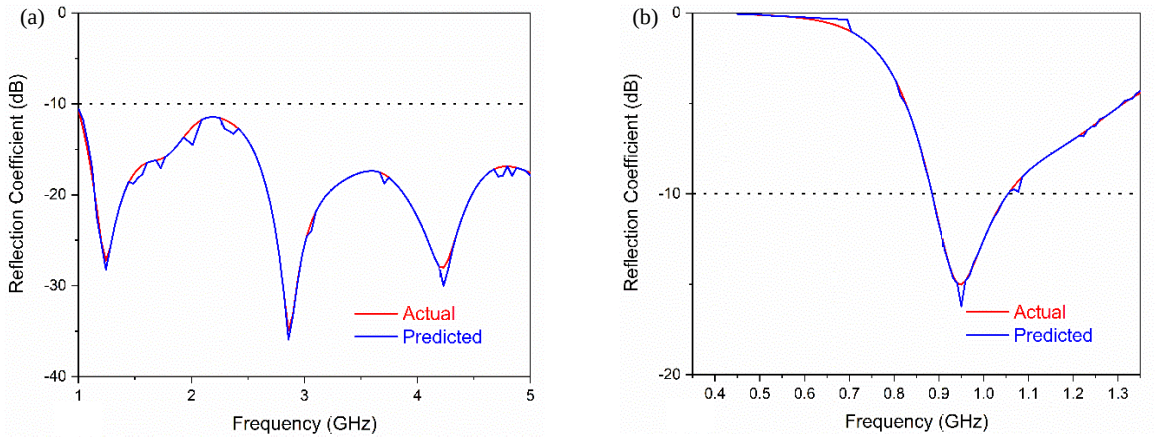

FIGURE 9. (a) Actual and predicted S_{11} for circular disc monopole antenna. (b) Actual and predicted S_{11} for wire monopole antenna.

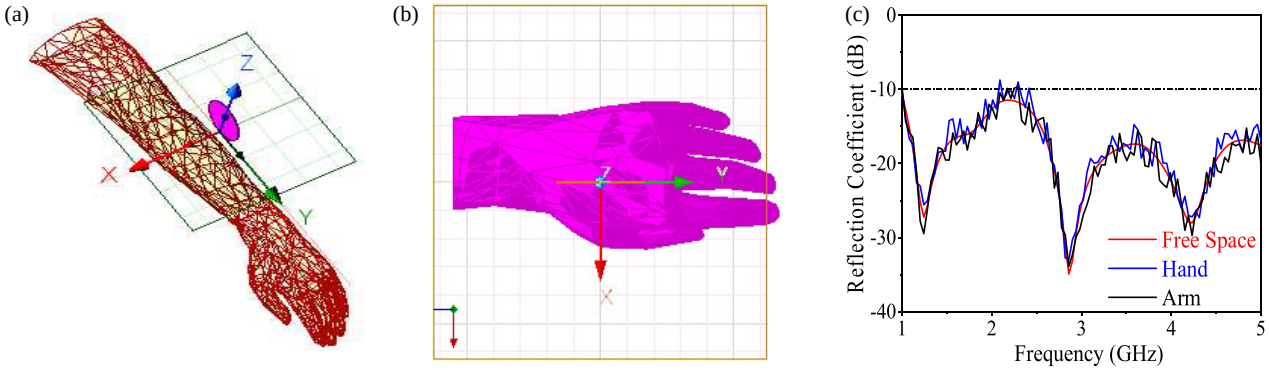

FIGURE 10. Circular disc monopole antenna SAR measurement setup in HFSS. (a) Hand and (b) arm, (c) reflection coefficient of circular disc monopole antenna with human phantom.

ulated due to time constraints on the SAR measurement simulation. The SAR values meet FCC and IEEE safety standards [26]. Figure 10(c) shows the circular disc monopole antenna's reflection coefficient with a human phantom. S_{11} values for the hand, arm, and open space were similar with very minor differences. Although it is not a design target in this study, energy efficiency is crucial for wearable antenna applications that require compactness, low power consumption, and user safety. Machine learning-optimized monopole designs utilize low-loss substrates and small geometries for efficient operation. Future work can include energy-aware design metrics for wearable and low-power applications within ML-based systems.

5. CONCLUSION

This research used a methodological approach to construct a machine-learning model for predicting geometric parameters and antenna categorization. The suggested model employed SFIS technique and utilized EONN classifier to achieve an accuracy of over 99.3%. The error rate of the SFIS-based geometric parameter estimation model is less than 4%. The suggested approach is also more efficient than existing techniques, with a training time of 13.255 seconds and a prediction speed of 7000 observations per second. Due to its high gain and improved bandwidth, the circular disc monopole antenna proposed in this work is suitable for wearable technology. Furthermore, the antenna design outperforms other designs, as evidenced by its higher SAR value. To account for new characteristics, future studies will investigate other machine-learning techniques for the same antenna design. For accurate antenna categorization and geometric parameter prediction, the suggested model (EONNC + SFIS) can be implemented in real time.

REFERENCES

[1] Yahya, M. S., S. Soeung, S. K. A. Rahim, U. Musa, S. S. B. Hashwan, and M. A. Haque, "Machine learning-optimized compact frequency reconfigurable antenna with RSSI enhancement for long-range applications," *IEEE Access*, Vol. 12, 10 970–10 987, 2024.

[2] Rizwan, S., K. V. P. Kumar, and A. J. Alazemi, "A compact textile monopole antenna for monitoring the healing of bone fractures using un-supervised machine learning algorithm," *IEEE Access*, Vol. 11, 101 195–101 204, 2023.

[3] Zheng, X., F. Meng, Y. Tian, and X. Zhang, "Design of monopole antennas based on progressive Gaussian process," *International Journal of Microwave and Wireless Technologies*, Vol. 15, No. 2, 255–262, 2023.

[4] Huang, H., X.-S. Yang, and B.-Z. Wang, "Machine-learning-based generative optimization method and its application to an

antenna decoupling design," *IEEE Transactions on Antennas and Propagation*, Vol. 71, No. 7, 6243–6248, 2023.

[5] Ramasamy, R. and M. A. Bennet, "Optimizable KNN and ANFIS algorithms development for accurate antenna parameter estimation," *Progress In Electromagnetics Research C*, Vol. 142, 207–218, 2024.

[6] Ramasamy, R. and M. A. Bennet, "An efficient antenna parameters estimation using machine learning algorithms," *Progress In Electromagnetics Research C*, Vol. 130, 169–181, 2023.

[7] Sharma, Y., H. H. Zhang, and H. Xin, "Machine learning techniques for optimizing design of double T-shaped monopole antenna," *IEEE Transactions on Antennas and Propagation*, Vol. 68, No. 7, 5658–5663, 2020.

[8] Sharma, Y., X. Chen, J. Wu, Q. Zhou, H. H. Zhang, and H. Xin, "Machine learning methods-based modeling and optimization of 3-D-printed dielectrics around monopole antenna," *IEEE Transactions on Antennas and Propagation*, Vol. 70, No. 7, 4997–5006, 2022.

[9] Wu, Q., W. Chen, C. Yu, H. Wang, and W. Hong, "Machine-learning-assisted optimization for antenna geometry design," *IEEE Transactions on Antennas and Propagation*, Vol. 72, No. 3, 2083–2095, 2024.

[10] Shah, A. H., K. Ghosh, and P. N. Patel, "Modeling and optimization of CPW-fed E-textile antenna using machine learning algorithms," *Progress In Electromagnetics Research C*, Vol. 130, 31–42, 2023.

[11] Pandi Ravichandran, V. and N. Velayudham, "On the performance investigation of a low profile UWB antenna backed with conjointly connected sickle shaped AMC structure for on-/off body communications," *Frequenz*, Vol. 79, No. 7–8, 2025.

[12] Nakmouche, M. F., A. Allam, D. E. Fawzy, and D.-B. Lin, "Development of a high gain FSS reflector backed monopole antenna using machine learning for 5G applications," *Progress In Electromagnetics Research M*, Vol. 105, 183–194, 2021.

[13] Choo, J., T. H. A. Pho, and Y.-H. Kim, "Machine learning technique to improve an impedance matching characteristic of a bent monopole antenna," *Applied Sciences*, Vol. 11, No. 22, 10829, 2021.

[14] Shi, D., C. Lian, K. Cui, Y. Chen, and X. Liu, "An intelligent antenna synthesis method based on machine learning," *IEEE Transactions on Antennas and Propagation*, Vol. 70, No. 7, 4965–4976, 2022.

[15] Ganesh, T. and D. Chaturvedi, "Design of wearable monopole antenna sensor for breast tumor detection," in *2024 IEEE Wireless Antenna and Microwave Symposium (WAMS)*, 1–4, Visakhapatnam, India, 2024.

[16] Zhao, M., A. Riaz, I. M. Saied, Z. Shami, and T. Arslan, "Dual-planar monopole antenna-based remote sensing system for microwave medical applications," *Sensors*, Vol. 24, No. 2, 328, 2024.

[17] Saad, A. A. R., W. M. Hassan, and A. A. Ibrahim, "A monopole antenna with cotton fabric material for wearable applications," *Scientific Reports*, Vol. 13, No. 1, 7315, 2023.

[18] Sam, P. J. C., U. Surendar, U. M. Ekpe, M. Saravanan, and P. S. Kumar, "A low-profile compact EBG integrated circular monopole antenna for wearable medical application," in *Smart Antennas: Latest Trends in Design and Application*, 301–314, Springer International Publishing, Cham, 2022.

[19] Abdelghany, M. A., M. I. Ahmed, A. A. Ibrahim, A. Desai, and M. F. Ahmed, "Textile antenna with dual bands and SAR measurements for wearable communication," *Electronics*, Vol. 13, No. 12, 2251, 2024.

[20] Chatterjee, D. and A. K. Kundu, "Implementation of machine learning for the design of spiral shaped multiband monopole antenna for MICS/IEEE802.11a/IEEE802.11b applications," *Journal of Electromagnetic Waves and Applications*, Vol. 39, No. 3, 318–343, 2025.

[21] Yahya, M. S., S. Soeung, S. K. A. Rahim, T. K. Geok, and U. Musa, "Machine learning-optimized wearable antenna for LoRa localization," *IEEE Access*, Vol. 12, 139 237–139 252, 2024.

[22] Hamdi, A. and A. Balti, "Experimental study on designing smart antenna sensor networks and modelling management energy consumption for intelligent systems of internet of medical things," *Journal of Information and Telecommunication*, Vol. 9, No. 3, 357–381, 2025.

[23] Leonardi, O., M. G. Pavone, G. Sorbello, A. F. Morabito, and T. Isernia, "Compact single-layer circularly polarized antenna for short-range communication systems," *Microwave and Optical Technology Letters*, Vol. 56, No. 8, 1843–1846, 2014.

[24] Rajavel, V. and D. Ghoshal, "A compact triband antenna using artificial magnetic conductor for wireless body area network communicationsFront," *Wireless Networks*, Vol. 29, No. 6, 2773–2795, 2023.

[25] Institute of Electrical and Electronics Engineers (IEEE). IEEE Standard for Safety Levels with Respect to Human Exposure to Radio Frequency Electromagnetic Fields, 3 kHz to 300 GHz. IEEE Std C951-2005 (Revision of IEEE Std C951-1991), 1–238, 2006.